



Published in final edited form as:

J Orthop Res. 2011 March ; 29(3): 340–346. doi:10.1002/jor.21259.

Organ-Level Histological and Biomechanical Responses from Localized Osteoarticular Injury in the Rabbit Knee

Tanawat Vaseenon, MD¹, Yuki Tochigi, MD, PhD¹, Anneliese D. Heiner, PhD^{1,2}, Jessica E. Goetz, PhD^{1,2}, Thomas E. Baer, BA¹, Douglas Fredericks, BS¹, James A. Martin, PhD^{1,2}, M. James Rudert, PhD¹, Stephen L. Hillis, PhD³, Thomas D. Brown, PhD^{1,2}, and Todd O. McKinley, MD¹

¹Department of Orthopaedics and Rehabilitation, University of Iowa

²Department of Biomedical Engineering, University of Iowa

³Center for Research in the Implementation of Innovative Strategies in Practice (CRIISP), VA Iowa City Medical Center, and Department of Biostatistics, the University of Iowa

Abstract

The processes of whole-joint osteoarthritis development following localized joint injuries are not well understood. To demonstrate this local-to-global linkage, it was hypothesized that a localized osteoarticular injury in the rabbit knee would not only cause biomechanical and histological abnormalities in the involved compartment, but also concurrent histological changes in the non-involved compartment. Twenty rabbits had an acute osteoarticular injury that involved localized joint incongruity (a 2 mm osteochondral defect created in the weight-bearing area of the medial femoral condyle), while another twenty received control sham surgery. At the time of sacrifice at eight or sixteen weeks post-surgery, the experimental knees were subjected to sagittal-plane laxity measurement, followed by cartilage histo-morphological evaluation using the Mankin score. The immediate effects of defect creation on joint stability and contact mechanics were explored in concomitant rabbit cadaver experimentation. The injured animals had cartilage histological scores significantly higher than in the sham surgery group ($p < 0.01$) on the medial femoral, medial tibial, and lateral femoral surfaces (predominantly on the medial surfaces), accompanied by slight (mean 20%) increase of sagittal-plane laxity. Immediate injury-associated alterations in the medial compartment contact mechanics were also demonstrated. Localized osteoarticular injury in this survival animal model resulted in global joint histological changes.

Keywords

joint injury; osteoarthritis; cartilage histology; rabbit knee; osteochondral defect

Introduction

Post-traumatic osteoarthritis (OA) manifests as progressive degeneration of the whole joint following a traumatic injury. The pathogenesis of this disorder is multifactorial¹, including acute mechanical damage sustained by the cartilage at the time of the injury, and chronic abnormal loading patterns that ensue due to decrements in articular surface congruity, stability, and alignment. While some of these injury-related factors are localized within single components of the joint, end stage post-traumatic OA is characterized by destructive

changes expanding to affect the joint in its entirety. These observations suggest that there are organ-level mechanisms by which local articular surface injuries lead to whole-joint degeneration. However, the pathomechanisms responsible for disease progression to organ level have not been well documented.

It has long been a well-accepted concept that an articular surface incongruity results in local cartilage over-loading that leads to degeneration. However, laboratory experiments in static cadaveric preparations have documented only modest increases in cartilage contact stresses, in the face of substantial incongruities^{2,3}. Dynamically, in cadaveric preparations of incongruous joints subjected to a physiologic motion/load sequence, although the increase in contact stresses was modest, several-fold increases in local cartilage loading rates have been demonstrated^{4,5}. These observations imply that articular surface incongruity presumably causes pathogenic dynamic aberrations in local joint contact mechanics as well as in whole-joint kinematics. This dynamic mechanism may be an important co-factor that contributes to progression of whole-joint cartilage degeneration from a localized osteoarticular injury.

This study was designed to investigate *in vivo* the association between localized osteoarticular injury and whole-joint OA development. In a survival animal experiment, an osteochondral defect in the primary weight-bearing region of the medial femoral condyle was created in the rabbit knee, and the whole-organ short-to-mid-term effects were explored. The immediate biomechanical effects of the defect creation were also studied in concomitant rabbit knee cadaver experiments. The hypothesis was that a localized osteoarticular injury in the medial femoral primary weight-bearing surface would cause whole-joint cartilage degeneration, along with biomechanical abnormalities that plausibly explain the disease progression.

Methods

Survival Experimentation

Forty mature New Zealand white rabbits (12 to 15 months old, average weight 4.5 kilograms) were subjected to surgery in the left knee. The surgery was performed under general anesthesia, with the animal in the prone position, in order to approach the primary contact region of the medial femoral condyle at 135 degrees of knee flexion (representative habitual physiologic knee position for rabbits placed in cage confinement^{6,7}) (Figure 1). A medial popliteal longitudinal skin incision was made, and the posteromedial joint capsule was exposed through the intermuscular plane between the semimembranosus and medial gastrocnemius. The gastrocnemius tendon was retracted laterally, with the femoral insertion left intact. The joint capsule was then incised longitudinally. In twenty animals, a circular osteochondral defect that reached subchondral bone, typically 1 to 1.5 mm depth, was created at the center of the posterior femoral surface (the incongruous injury group). Using a 2 mm dermal biopsy punch, cartilage and bone in a sharp circular cut were simultaneously removed (like harvesting a cylindrical osteochondral allograft). The other twenty animals received the posterior arthrotomy alone (the sham surgery control group). All animals were allowed free cage activity and an *ad lib* diet throughout the testing period. For each treatment group, half of the animals were sacrificed at eight weeks, and the other half at sixteen weeks. The surgery, euthanasia, and other animal care were performed following a protocol approved by the Institutional Animal Care and Use Committee.

At the time of sacrifice, the experimental knees were subjected to sagittal-plane stability measurement using a custom loading fixture designed for the rabbit knee⁸ (Figure 2A). In this device, the rabbit was placed in the supine position, with the femur secured vertically using percutaneous half-pins. The tibia was secured with transverse pins to a horizontal leg holder, with the knee held at 90 degrees flexion. The leg holder was in turn attached to a

stepper-motor-driven actuator. The actuator applied cyclic anterior and posterior knee drawer displacement at a test speed of 1 mm/sec, with limits for direction reversal set as ± 75 N or ± 3 mm, whichever was reached first. Force-vs-displacement data during loading were continuously recorded. The test sequence consisted of four discrete cycles of preconditioning (during which the “zero” displacement position was adjusted), followed by four continuous cycles of preconditioning, and then four continuous loading cycles for data collection. The knee drawer force-vs-displacement relationship was typically characterized by a sigmoid curve (Figure 2B). The length of the central flat portion of the curve, within the range of ± 7.5 N of drawer force, was defined as the neutral-zone length (NZL). The neutral-zone length data for each of the four continuous data collection cycles were averaged.

The experimental knees were then prepared for cartilage histological evaluation, following OsteoArthritis Research Society International (OARSI) guidelines⁹. For each joint, sagittal histological sections (stained with Safranin O-Fast Green) were created for the medial/lateral femoral condyles and the medial/lateral tibial plateaus. High magnification digital images were then captured at 743,028 pixels/mm² resolution, using a QICAM[®] 12-bit camera (QImaging[™], Surrey, British Columbia, Canada) mounted on a microscope (Model BX60, Olympus Co., Tokyo, Japan) with a 4 \times objective, coupled with a stepper-motor-driven stage (Prior Scientific Inc., Rockland, Maryland, USA). Individual high-resolution image fields were concatenated using Image-Pro[®] (Media Cybernetics Inc., Silver Spring, Maryland, USA) to produce (stitched) full-cartilage-thickness osteochondral images. For each section, the central part (approximately a 1 mm-width) of the joint surface’s primary weight-bearing region (where cartilage was thickest) was cropped, and a unique identification number was randomly assigned. In the case of medial femoral sections for the incongruous injury group, a representative region adjacent to the surgically-created defect (either anterior or posterior, at least 0.5 mm away from the defect edge) was selected. Cartilage histology was evaluated in a blinded fashion, using Mankin’s Histological Histochemical Grading Scale (HHGS)¹⁰. The femoral and tibial surfaces in both the medial and lateral compartments were rated individually. Two experienced orthopaedic surgeons (TV, YT) rated these blinded images. Each observer individually scored each image twice (i.e., a total of four scores per image), and the mean value was recorded as a final score.

Cadaver Experimentation

The immediate effects of the same osteoarticular injury on contact mechanics were assessed in seven fresh rabbit cadaver knees. These specimens were dissected free of skin and surrounding tissue, with the major ligaments and menisci left intact. The distal femur and proximal tibia of each joint were potted into separate polymethylmethacrylate (PMMA) blocks, with the knee held at approximately 135 degrees of flexion. The specimen was then mounted in a custom-designed loading device (Figure 3A) actuated by an electromechanical materials testing machine (MTS Insight 1, MTS Systems Corp., Eden Prairie, Minnesota, USA). Flexion/extension of the knee was adjustable in five-degree increments. Adduction/abduction about the axis aligned with the center of the knee was left unrestricted, allowing the joint to align naturally while the load was being applied. To measure contact stresses in the medial compartment, a 10 mm \times 30 mm rectangle pressure sensitive film (Low Range Prescale[®], Fujifilm Co., Tokyo, Japan) was inserted into the knee beneath the meniscus, through a small arthrotomy. Axial compression was linearly increased over two seconds to a physiologic-level force¹¹ (100 N), held constant for two seconds, and then linearly decreased back to zero. For each joint, with the joint surface intact (the baseline condition), contact stresses in the medial compartment were first measured at five flexion angles ranging from 125 to 145 degrees in 5-degree increments. Subsequently, a 2 mm diameter osteochondral defect was created (the defect condition) in a manner identical to that in the survival experiment, and the above-described contact stress measurement protocol was

repeated. Contact stress data captures at the flexion angle showing the greatest contact circumferentially around the defect region were chosen for quantitative analysis. Films were digitized at a resolution of 118 pixels per centimeter, and were analyzed using a purpose-written program implemented in MATLAB (MathWorks™ Inc., Natick, Massachusetts, USA). These analyses used a calibration curve generated using a 6.35 mm diameter rigid platen and eight known stress levels, to convert the pixel intensity values to peak contact stress values. This analysis program identified the outline(s) of the contact patch (based on an intensity threshold), and then calculated the total contact area, the peak contact stress value, and the maximal sagittal- and coronal-direction spans of the contact patch (Figure 3B).

The immediate effects of defect creation on sagittal-plane stability were assessed in seven fresh rabbit cadaver knees, in a manner identical to that described for the survival animal experiment. Each knee, with the primary weight-bearing region of its medial femoral surface being exposed by means of posterior arthrotomy, was tested with the articular surface intact (baseline) and then immediately after defect creation.

Statistical Analysis

In the survival experiment, because the number of animals for each combination of treatment (incongruous injury versus sham surgery control) and test period (8 versus 16 weeks) was relatively small ($n = 10$), a nonparametric test (the Wilcoxon rank-sum test) analogous to the conventional two-sample t -test was used to test for equality of treatment means, using the pooled eight- and sixteen-week data ($n = 20$, per group). This test was applied individually to the four respective surface histological scores and to the stability measure. Exploratory comparisons were performed between test periods ($n = 10$ per subgroup) within each treatment group, again using the rank-sum test. Data from cadaver loading tests (both contact mechanics and stability) were statistically compared between the baseline and defect conditions, again using the Wilcoxon signed-rank test. Because of the small sample size (hence low power) and to avoid inflation of the overall type I error rate, these tests were considered to be exploratory. All tests were performed using a significance level of alpha set at 0.05.

Results

In histological analysis for the survival study (Figure 4), statistical comparisons between treatment groups (for which the data from the eight- and sixteen-week animals were pooled) indicated that the incongruous injury group had cartilage degeneration (histological scores significantly higher than in the sham surgery control group) for the medial femoral surface ($p < 0.0001$), the medial tibial surface ($p < 0.0001$), and the lateral femoral surface ($p = 0.0011$). For the medial tibial surface, degeneration reached the middle- to deep-zone (HHGS = 4) in most cases, in both the eight- and sixteen-week animals. For the medial femoral surface, similarly severe degeneration was identified only in the sixteen-week animals (seven out of ten animals), with the difference between the time-period sub-groups being close to statistically significant ($p = 0.072$). For the lateral femoral surface, degenerative changes were relatively mild (HHGS < 4) in all cases. Appreciable remodeling of bone and cartilage in the defect region (reaching the level of articular surface) was not identified in any knees in the incongruous injury group.

In the survival animal stability test (Figure 5A), the neutral-zone length in the incongruous injury group (including both eight- and sixteen-week animals) was significantly longer ($p = 0.014$) than in the sham surgery group, indicating that the incongruous knees had increased sagittal-plane laxity at the time of sacrifice. The mean increase with respect to the sham surgery group was 20 percent. No statistical difference between time-periods was evident.

By contrast, in cadaver experimentation (Figure 5B), sagittal-plane stability remained nearly equivalent before versus after defect creation ($p = 0.94$, root-mean-square difference = 7.4%).

In the cadaver contact mechanics test, changes of the shape of contact patch (Figure 3B) associated with defect creation showed significant increases of the coronal and sagittal spans ($p = 0.031$, for both, Figure 6). This occurred, however, without an accompanying increase of engaged contact area ($p = 0.47$), suggesting that contact stresses were simply shifted from the defect area onto the adjacent regions of the joint surface. Slight increase (up to +23.5%) of peak contact stress value with defect creation occurred in six out of the seven specimens, with the difference close to statistical significance ($p = 0.078$).

Discussion

The present study explored whole-organ cartilage responses from localized osteoarticular injury in the rabbit knee *in vivo*, for the first time simultaneously with the associated changes in the joint mechanics. Use of the posterior surgical approach allowed creating an isolated osteochondral defect in the most heavily weight-bearing posterior region of the rabbit medial femoral condyle, without damaging the surrounding cartilage. This surgical insult necessarily involved intraarticular bleeding from incised capsule and bone marrow, and it needs to be borne in mind that cartilage is sensitive to exposure to blood^{12,13}. However, this hemoarthrosis is actually consistent with clinical conditions after traumatic osteoarticular injuries or surgical intervention for them. The survival model, which involved a relatively small solitary osteoarticular injury on the medial femoral surface (a 2 mm full-thickness osteochondral defect in the weight-bearing region), exhibited appreciable cartilage degeneration in the medial compartment, both near the femoral defect itself and on the opposing tibial surface. In addition to this local compartment degeneration, modest but significant degenerative changes in cartilage histology were identified at a remote location (on the lateral femoral surface). As hypothesized, a localized osteoarticular injury influenced whole-joint cartilage conditions in the present rabbit knee model. This is very different from whole-joint arthritis secondary to whole-joint insult, as in the murine knee fracture model of Fruman et al.¹⁴. By implication, there were organ-level mechanism(s) by which a localized osteoarticular injury induced propagation of cartilage degeneration to the whole-joint level.

Regarding the local (medial) compartment degeneration, in a previous horse knee model of osteoarticular injury¹⁵, a larger-diameter (9 to 21 mm) circular defect created on the medial femoral condyle caused cartilage degeneration on the opposing medial tibial plateau surface, with the degrees of degeneration higher when a defect was larger. In a rabbit knee model^{16,17}, incongruous osteoarticular injury on the medial femoral condyle was modeled by creating a 3 mm-wide longitudinal osteochondral fragment through an anterior arthrotomy, with the fragment fixed at a 2 or 5 mm proximally-displaced “step-off” position. In this model, joints with a 5 mm step-off incongruity developed degeneration across the whole joint, including the opposing medial tibial cartilage.¹⁷ (Note: Such phenomena were not evident in the 2 mm step-off group¹⁶. However, since the femoral surface accessible through an anterior arthrotomy is typically the inferior aspect rather than posterior, success in positioning the step-off incongruity in the primary habitual weight-bearing surface may have been different between groups.) Observations in those models are consistent with the present study, in that femoral incongruity caused degeneration on the opposing tibial surface. However, the percentage of the habitual weight-bearing surface having a step-off incongruity appears to be smaller in the present study (with a 2 mm circular defect) than in those models. In the rabbit cadaver contact mechanics test, the immediate effects of defect creation did not involve dramatic elevation of peak local contact stress, as previously documented in a canine osteochondral defect knee model². However, the morphology of the

contact patch changed significantly with defect creation, indicating that the incongruous injury knees in the survival experiment must have had similarly aberrant contact mechanics in the medial compartment. At a microscopic level, it has been demonstrated that cartilage opposing a defect surface is subjected to supra-physiologic deformation associated with the stress gradient at the boundary between contact and non-contact regions¹⁸. During joint motion, cartilage at that boundary is presumably also subjected to a supra-physiologically high-rate of deformation. Given that chondrocytes are very sensitive to loading rate¹⁹⁻²², such abnormal dynamic loading plausibly explains the medial compartmental degeneration in the survival experiment. In addition, redistribution of contact stresses from the habitual weight-bearing region to a less habitually loaded peripheral region may have affected the cartilage local mechanical milieu, causing adverse long-term effects²³. These dynamic mechanisms may have been responsible for the compartment degeneration accompanying the relatively small osteochondral defect in the present study.

Stability testing in the survival study demonstrated that the rabbit knees with the osteoarticular injury had modestly increased laxity at the time of sacrifice. However, such laxity was not identified in the rabbit cadaver stability test. Presumably, the increased laxity in the survival study therefore developed secondarily during the testing period, by biologically mediated mechanisms such as collagen fiber weakening caused by inflammatory cytokines^{24,25}. The extra surgical insult in the incongruous injury knees (i.e., defect creation) may have caused stronger acute inflammation compared to the control knees with otherwise identical surgical procedure. The resulting joint instability, along with abnormalities in the joint kinematics associated with the aberrant medial compartment contact mechanics (discussed above), probably contributed to whole-joint degenerative changes in cartilage histology, by causing instability events involving deleteriously high-rate cartilage loading⁵. Besides such biomechanical factors, it is likely that an organ-level biologic response to acute (surgical) osteoarticular injury also affected cartilage throughout the entire joint. Custers et al.²⁶, who reported remote-site cartilage degeneration in the rabbit knees with a 3.5 mm medial femoral defect (created through an anterior arthrotomy at an inferior location rather than posterior), linked the mechanism of remote degeneration with an organ-level biologic response as proposed by Saris and colleagues²⁷. According to this concept, loss of physiologic equilibrium between the structures in a synovial joint following an injury leads to abnormal production of a myriad of intra-articular factors, such as inflammatory cytokines or cellular components, which once in the synovial fluid affect the entire joint. Therefore, it would seem that the remote-site degenerative changes observed in this organ-level model were secondary to incongruity-associated biomechanical abnormalities, in concert with acute traumatic disturbance of organ-level physiologic homeostasis of the joint.

A limitation of this study was that cartilage degeneration was quantified purely with histological indices, which depend on subjective observer judgment. However, both observers repeated their measurements in a blinded fashion, and inter-observer and intra-observer reliabilities were high ($r > 0.9$, for both). The “whole-joint” histological evaluation was performed only in the femoro-tibial joints; the patello-femoral joint was not included. Lack of means to measure local inflammation precluded studying the contributions of inflammatory biological responses to the reported changes in cartilage histology and joint laxity. Further investigation is needed to clarify the mechanisms of the remote-site cartilage changes and increased joint laxity observed in the survival study. Finally, no statistically significant differences were detected between specimens observed at eight weeks versus sixteen weeks. Lack of significant time-dependence may have been due to the two time points having been too close together to discriminate the effects of time on degeneration, or to insufficient power to detect a meaningful effect size (the power was less than 33% for detecting a difference as large as a 0.5-fold standard deviation if the distributions were normally distributed). The lack of progression over the second eight weeks of the

experiment may also have been influenced by the rabbits being confined to cage activity, as opposed to moving in their natural environment.

In conclusion, the short- to mid-term whole-joint effects of an isolated localized osteoarticular injury in the weight-bearing surface of the rabbit knee medial femoral condyle involved degenerative changes in cartilage histology that occurred predominantly – but by no means exclusively – in the medial compartment. The mechanical data demonstrated that the accompanying localized incongruity involved onset of biomechanical abnormality consistent with causing cartilage degeneration. Presumably, the pathomechanisms operating in this rabbit knee model also contribute to development of post-traumatic OA after human osteoarticular injuries.

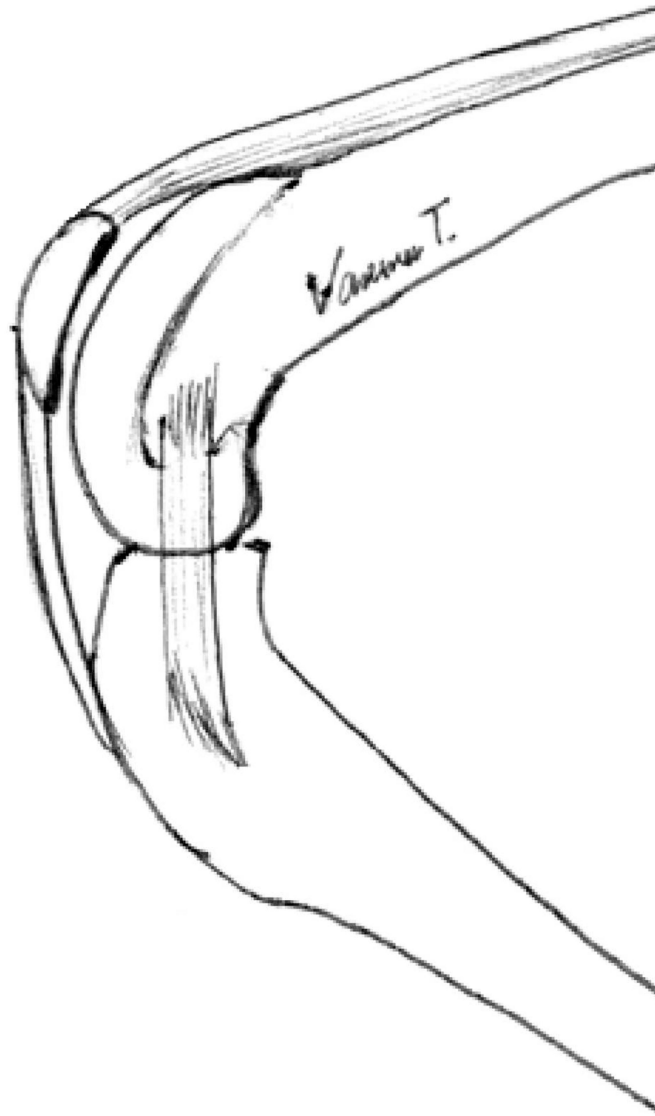
Acknowledgments

This research was supported by research grants from the CDC (R49 CCR721745) and the NIH (5 P50 AR048939 and 5 P50 AR055533).

References

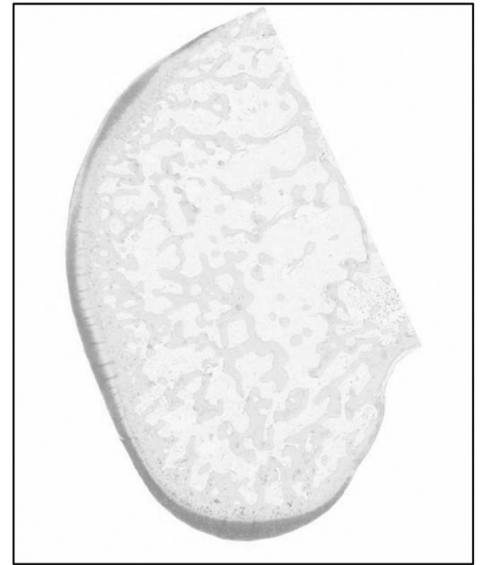
1. Buckwalter JA, Brown TD. Joint injury, repair, and remodeling: roles in post-traumatic osteoarthritis. *Clin Orthop Relat Res.* 2004; 7:16.
2. Brown TD, Pope DF, Hale JE, et al. Effects of osteochondral defect size on cartilage contact stress. *J Orthop Res.* 1991; 9:559–567. [PubMed: 2045983]
3. Koh JL, Wirsing K, Lautenschlager E, Zhang LO. The effect of graft height mismatch on contact pressure following osteochondral grafting: a biomechanical study. *Am J Sports Med.* 2004; 32:317–320. [PubMed: 14977653]
4. McKinley TO, Tochigi Y, Rudert MJ, Brown TD. The effect of incongruity and instability on contact stress directional gradients in human cadaveric ankles. *Osteoarthritis Cartilage.* 2008
5. McKinley TO, Tochigi Y, Rudert MJ, Brown TD. Instability-associated changes in contact stress and contact stress rates near a step-off incongruity. *J Bone Joint Surg Am.* 2008; 90:375–383. [PubMed: 18245598]
6. Mansour JM, Wentorf FA, Degoede KM. In vivo kinematics of the rabbit knee in unstable models of osteoarthritis. *Ann Biomed Eng.* 1998; 26:353–360. [PubMed: 9570218]
7. Newton PO, Woo SL, MacKenna DA, Akeson WH. Immobilization of the knee joint alters the mechanical and ultrastructural properties of the rabbit anterior cruciate ligament. *J Orthop Res.* 1995; 13:191–200. [PubMed: 7722756]
8. Heiner AD, Rudert MJ, McKinley TO, et al. In vivo measurement of translational stiffness of rabbit knees. *J Biomech.* 2007; 40:2313–2317. [PubMed: 17174958]
9. Pritzker KP, Gay S, Jimenez SA, et al. Osteoarthritis cartilage histopathology: grading and staging. *Osteoarthritis Cartilage.* 2006; 14:13–29. [PubMed: 16242352]
10. Mankin HJ, Dorfman H, Lippiello L, Zarins A. Biochemical and metabolic abnormalities in articular cartilage from osteo-arthritic human hips. II. Correlation of morphology with biochemical and metabolic data. *J Bone Joint Surg Am.* 1971; 53:523–537. [PubMed: 5580011]
11. Gushue DL, Houck J, Lerner AL. Rabbit knee joint biomechanics: motion analysis and modeling of forces during hopping. *J Orthop Res.* 2005; 23:735–742. [PubMed: 16022984]
12. Hooiveld M, Roosendaal G, Vianen M, et al. Blood-induced joint damage: longterm effects in vitro and in vivo. *J Rheumatol.* 2003; 30:339–344. [PubMed: 12563692]
13. Hooiveld M, Roosendaal G, Wenting M, et al. Short-term exposure of cartilage to blood results in chondrocyte apoptosis. *Am J Pathol.* 2003; 162:943–951. [PubMed: 12598327]
14. Furman BD, Strand J, Hembree WC, et al. Joint degeneration following closed intraarticular fracture in the mouse knee: a model of posttraumatic arthritis. *J Orthop Res.* 2007; 25:578–592. [PubMed: 17266145]
15. Convery FR, Akeson WH, Keown GH. The repair of large osteochondral defects. An experimental study in horses. *Clin Orthop Relat Res.* 1972; 82:253–262. [PubMed: 5011034]

16. Lefkoe TP, Walsh WR, Anastasatos J, et al. Remodeling of articular step-offs. Is osteoarthritis dependent on defect size? *Clin Orthop Relat Res.* 1995;253–265. [PubMed: 7634643]
17. Lefkoe TP, Trafton PG, Ehrlich MG, et al. An experimental model of femoral condylar defect leading to osteoarthritis. *J Orthop Trauma.* 1993; 7:458–467. [PubMed: 8229383]
18. Braman JP, Bruckner JD, Clark JM, et al. Articular cartilage adjacent to experimental defects is subject to atypical strains. *Clin Orthop Relat Res.* 2005:202–207. [PubMed: 15662325]
19. Chen CT, Burton-Wurster N, Lust G, et al. Compositional and metabolic changes in damaged cartilage are peak-stress, stress-rate, and loading-duration dependent. *J Orthop Res.* 1999; 17:870–879. [PubMed: 10632454]
20. Lee DA, Bader DL. Compressive strains at physiological frequencies influence the metabolism of chondrocytes seeded in agarose. *J Orthop Res.* 1997; 15:181–188. [PubMed: 9167619]
21. Morel V, Quinn TM. Cartilage injury by ramp compression near the gel diffusion rate. *J Orthop Res.* 2004; 22:145–151. [PubMed: 14656673]
22. Sah RL, Kim YJ, Doong JY, et al. Biosynthetic response of cartilage explants to dynamic compression. *J Orthop Res.* 1989; 7:619–636. [PubMed: 2760736]
23. Andriacchi TP, Koo S, Scanlan SF. Gait mechanics influence healthy cartilage morphology and osteoarthritis of the knee. *J Bone Joint Surg Am.* 2009; 91(Suppl 1):95–101. [PubMed: 19182033]
24. Kumar D, Fung W, Moore RM, et al. Proinflammatory cytokines found in amniotic fluid induce collagen remodeling, apoptosis, and biophysical weakening of cultured human fetal membranes. *Biol Reprod.* 2006; 74:29–34. [PubMed: 16148217]
25. Qi J, Fox AM, Alexopoulos LG, et al. IL-1beta decreases the elastic modulus of human tenocytes. *J Appl Physiol.* 2006; 101:189–195. [PubMed: 16627678]
26. Custers RJ, Creemers LB, van Rijen MH, et al. Cartilage damage caused by metal implants applied for the treatment of established localized cartilage defects in a rabbit model. *J Orthop Res.* 2009; 27:84–90. [PubMed: 18634008]
27. Saris DB, Dhert WJ, Verbout AJ. Joint homeostasis. The discrepancy between old and fresh defects in cartilage repair. *J Bone Joint Surg Br.* 2003; 85:1067–1076. [PubMed: 14516049]



A: Rabbit knee at a physiologic position

B: Sham (control)



C: Incongruity

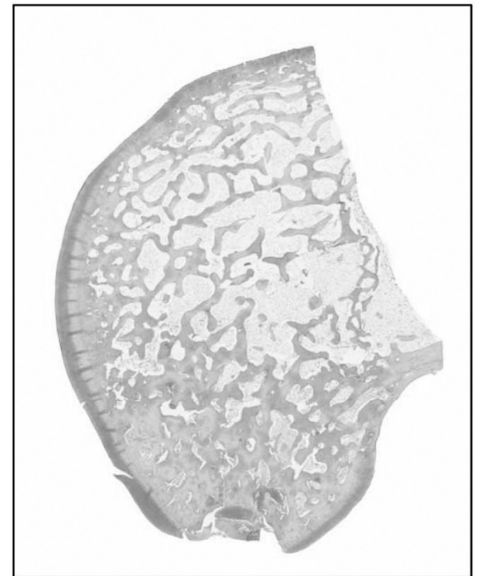


Figure 1.

A: The representative habitual physiologic knee position for rabbits in cage confinement is approximately 135 degrees of flexion. **B and C:** Histological findings at the time of sacrifice indicated that the defect was created at a region where articular cartilage was thickest.

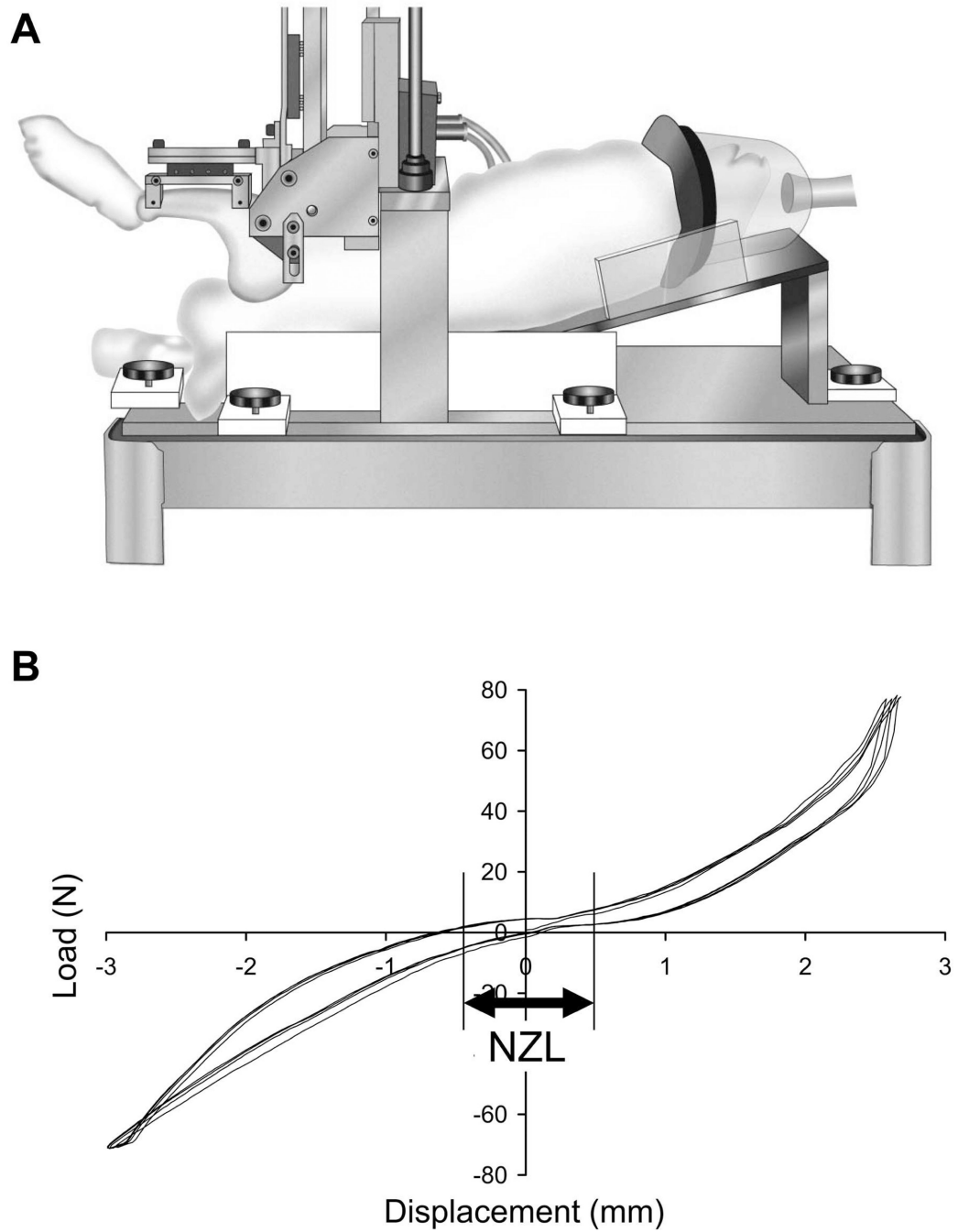


Figure 2.

A: Custom loading fixture for the sagittal-plane stability test. (Reprinted from Heiner et al., *J Biomech*, 2007⁸). **B:** Definition of the neutral-zone length (NZL: displacement between ± 7.5 N) from the load-displacement relationship.

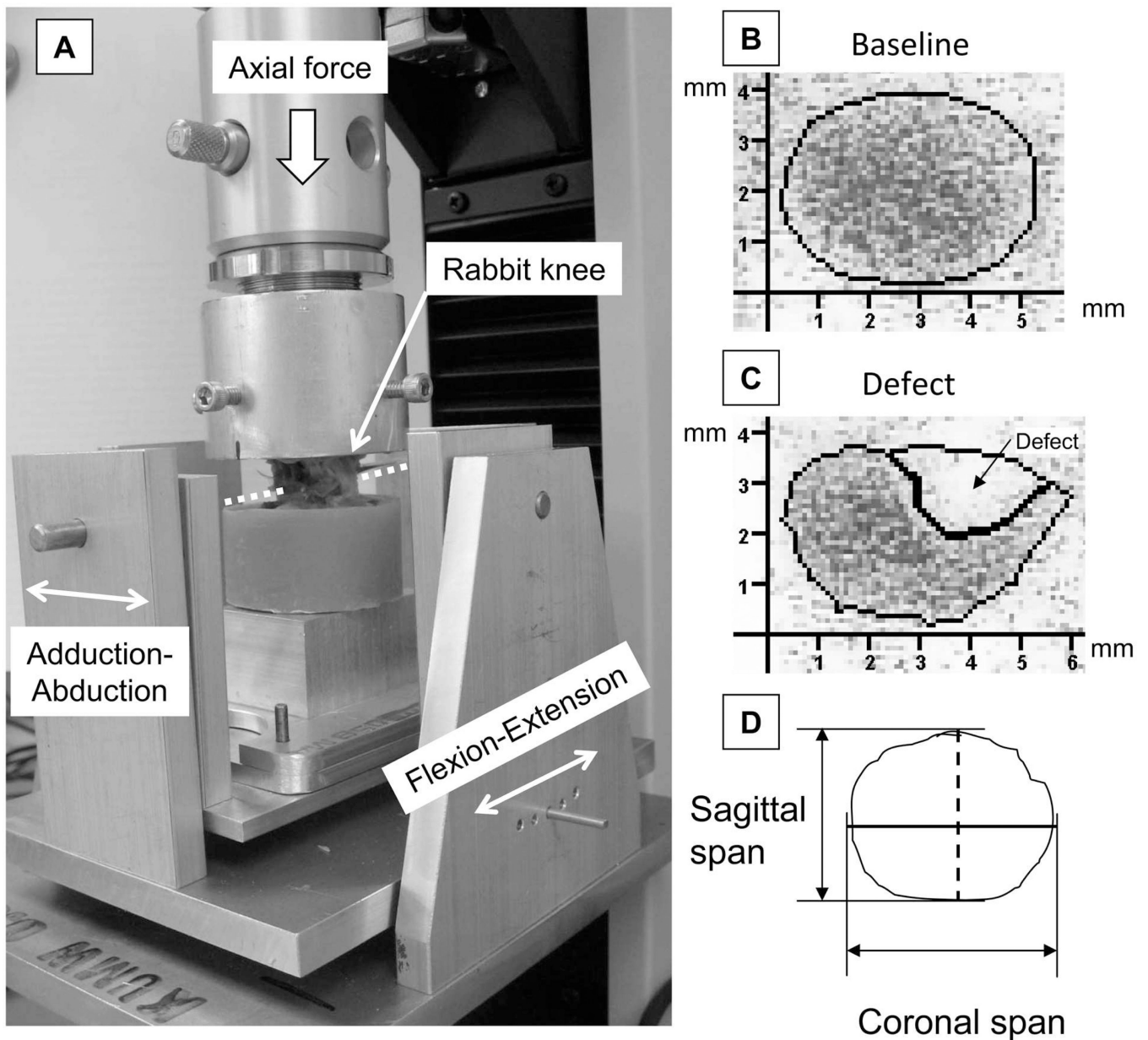


Figure 3.

A: Custom loading fixture for the contact mechanics test. The sagittal-plane position (flexion-extension) of the rabbit knee was adjustable in five-degree increments. The coronal-plane rotation (adduction-abduction) about the axis passing through the center of joint (dotted line) was unrestricted. **B and C:** Representative digitized Fujifilm images that indicate contact stress distribution in the medial compartment in a joint before defect creation (baseline) and contact stress redistributed after defect creation (defect). **D:** The longest spans of the contact patch in the sagittal direction (dashed black line) and in the coronal direction (solid black line) were registered.

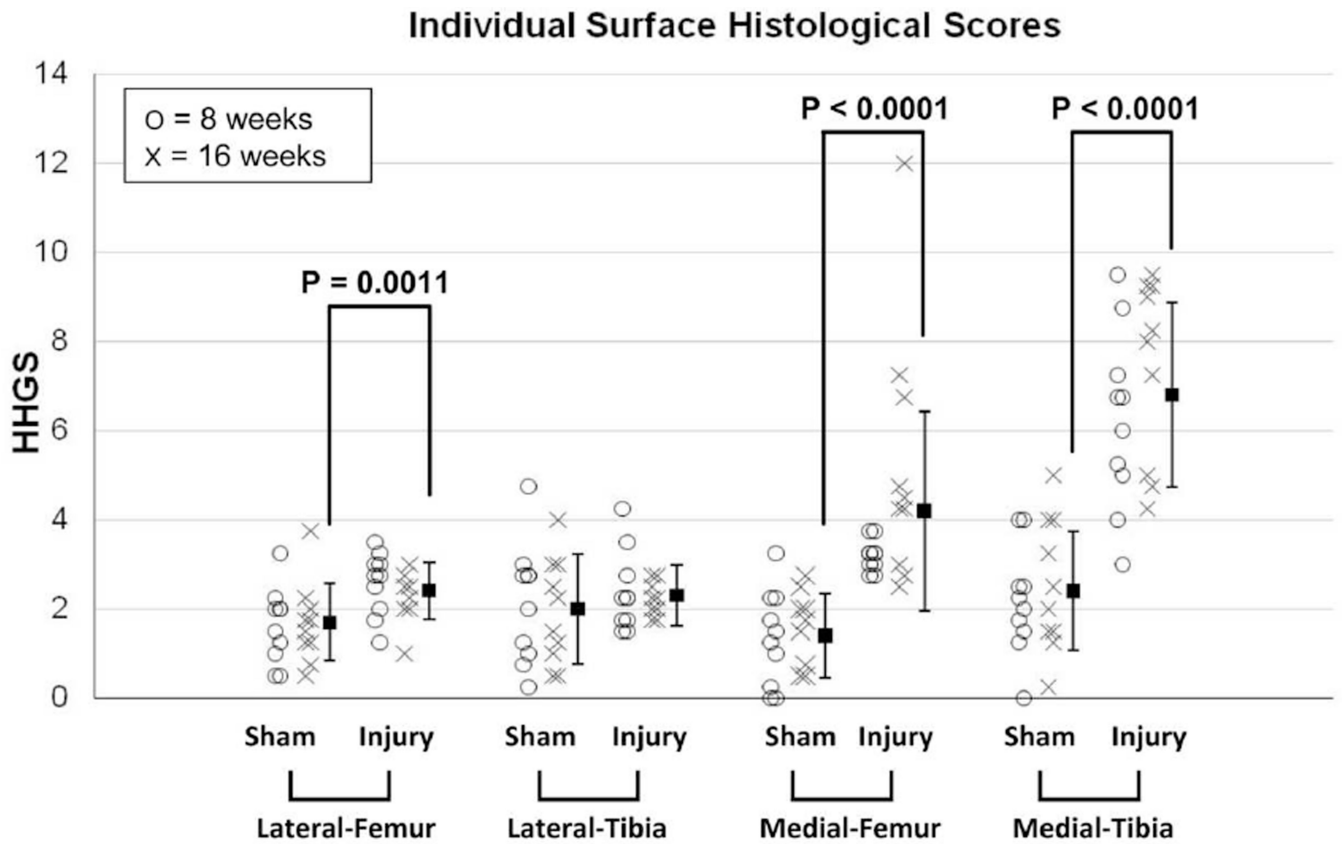


Figure 4. Results of histological evaluation for each individual joint surface. HHGS scores for each individual animal are plotted, along with the mean values (from both eight- and sixteen-week animals). The dispersion bars indicate standard deviations.

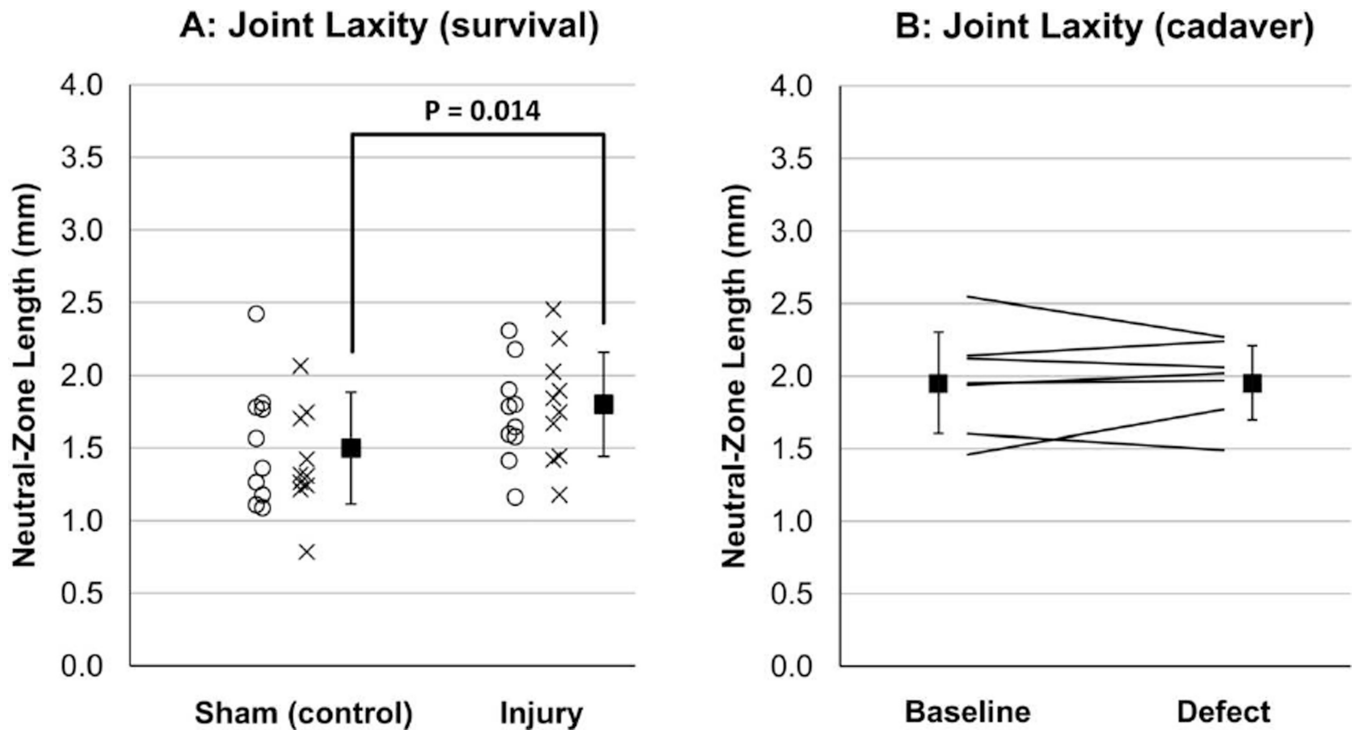


Figure 5.

A: Survival animal stability results. Individual-animal data are plotted for the sham surgery (control) and incongruous injury groups, along with the mean and standard deviation for each group (from both eight-week and sixteen-week animals). **B:** Cadaver specimen stability results. Corresponding individual-specimen data are plotted before (baseline) and after defect creation, along with the mean and standard deviation for each condition.

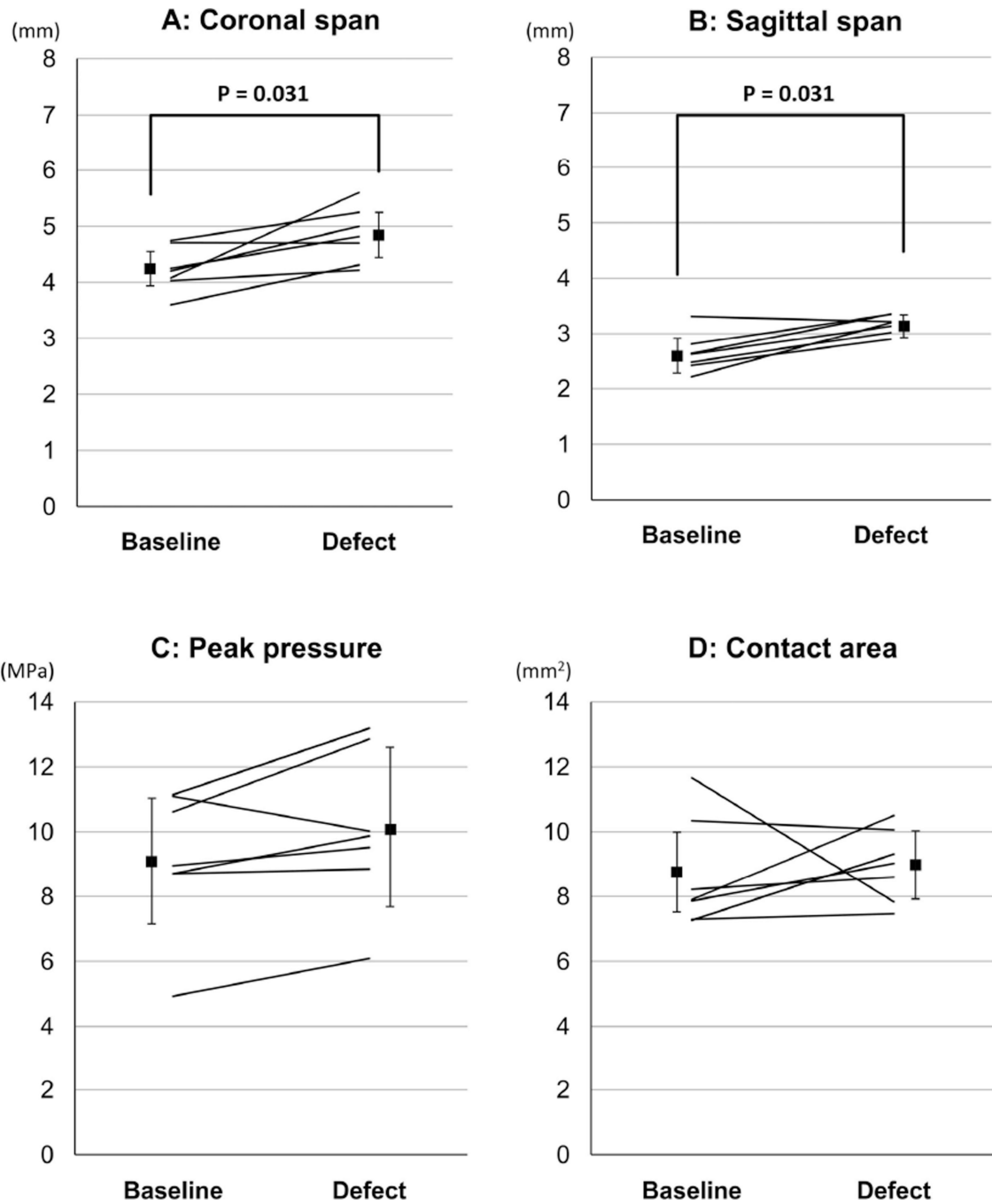


Figure 6. Cadaver specimen contact stress results. Corresponding individual-specimen data are plotted before (baseline) and after defect creation, along with the mean and standard deviation for each condition.